Oxidation and crack nucleation/growth in an air-plasma-sprayed thermal barrier coating with NiCrAlY bond coat

Chen, W. R.; Wu, Xijia; Marple, B. R.; Patnaik, P. C.

Publisher's version / Version de l'éditeur:
https://doi.org/10.1016/j.surfcoat.2004.06.027
Surface & Coatings Technology, 197, 1, pp. 109-115, 2005-07-01

Available online at www.sciencedirect.com
SCIENCE DIRECT
Surface & Coatings Technology 197 (2005) 109–115
SURFACE & COATINGS TECHNOLOGY
www.elsevier.com/locate/surfcoat

Oxidation and crack nucleation/growth in an air-plasma-sprayed thermal barrier coating with NiCrAlY bond coat

W.R. Chen[a,*], X. Wu[a], B.R. Marple[b], P.C. Patnaik[a]

[a]*Institute for Aerospace Research, National Research Council of Canada, 1200 Montreal Road, Bldg M-13, Ottawa, Ontario, Canada, K1A 0R6*
[b]*Industrial Materials Institute, National Research Council of Canada, Boucherville, Québec, Canada, J4B 6Y4*

Received 11 March 2004; accepted in revised form 14 June 2004
Available online 14 August 2004

Abstract

The oxidation behavior of an air-plasma-sprayed thermal barrier coating (APS-TBC) system was investigated in both air and low-pressure oxygen environments. It was found that mixed oxides, in the form of $(Cr,Al)_2O_3 \cdot Ni(Cr,Al)_2O_4 \cdot NiO$, formed heterogeneously at a very early stage during oxidation in air, and in the meantime, a layer of predominantly Al_2O_3 grew rather uniformly along the rest of the ceramic/bond coat interface. The mixed oxides were practically absent in the TBC system when exposed in the low-pressure oxygen environment, where the TBC had a longer life. Through comparison of the microstructures of the APS-TBC exposed in air and low-pressure oxygen environment, it was concluded that the mixed oxides played a detrimental role in causing crack nucleation and growth, reducing the life of the TBC in air. The crack nucleation and growth mechanism in the air-plasma-sprayed TBC is further elucidated with emphasis on the $Ni(Cr,Al)_2O_4$ and NiO particles embedded in the chromia.

Keywords: TBC; Bond coat; NiCrAlY; Oxidation; Cracks

1. Introduction

Thermal barrier coating (TBC) systems, which consist of an yttria partially stabilized zirconia ZrO_2–8%Y_2O_3 (ceramic) top coat and a metallic bond coat deposited onto a superalloy substrate, are favorably used as protective coatings on hot section components in advanced gas turbine engines to withstand increased inlet temperatures and thus improve engine performance [1]. Failure of a TBC system is often associated with oxidation of the metallic bond coat at elevated temperatures via formation of a thermally grown oxide (TGO) layer by depletion of aluminum from the bond coat [2–8]. In past work, it was observed that plasma-sprayed TBCs failed by spallation of the ceramic coat near the original ceramic/bond coat interface but mostly within the ceramic layer [9–12], whereas EB-PVD-produced TBCs failed at the interface between the TGO and the bond coat [13,14]. The TBC failure could be attributed, in part, to the biaxial compressive stress state built up at the interface between the ceramic top coat and the bond coat during cooling from elevated temperatures to the ambient temperature due to thermal expansion mismatch between the two constituents [2,5]. These stresses could increase progressively, cycle by cycle, as a result of the reduced deformability of the bond coat [2]. In addition, the biaxial in-plane compressive stresses could produce a tensile stress normal to the nominal coating plane at locations where local undulation of the interface was present. These tensile stresses, acting on the pre-existing flaws and defects, would promote crack initiation and delamination in the coating system [2,15–18]. Finite-element analyses have shown that the stresses in a TBC increase with a growing TGO layer [19–21].

Even though a general understanding of TBC failure in association with TGO formation and thermal mismatch-induced stress has been achieved, the specific crack

* Corresponding author. Tel.: +1 613 993 4321; fax: +1 613 990 7444.
E-mail address: weijie.chen@nrc-cnrc.gc.ca (W.R. Chen).

0257-8972/$ - see front matter © 2004 Elsevier B.V. All rights reserved.
doi:10.1016/j.surfcoat.2004.06.027

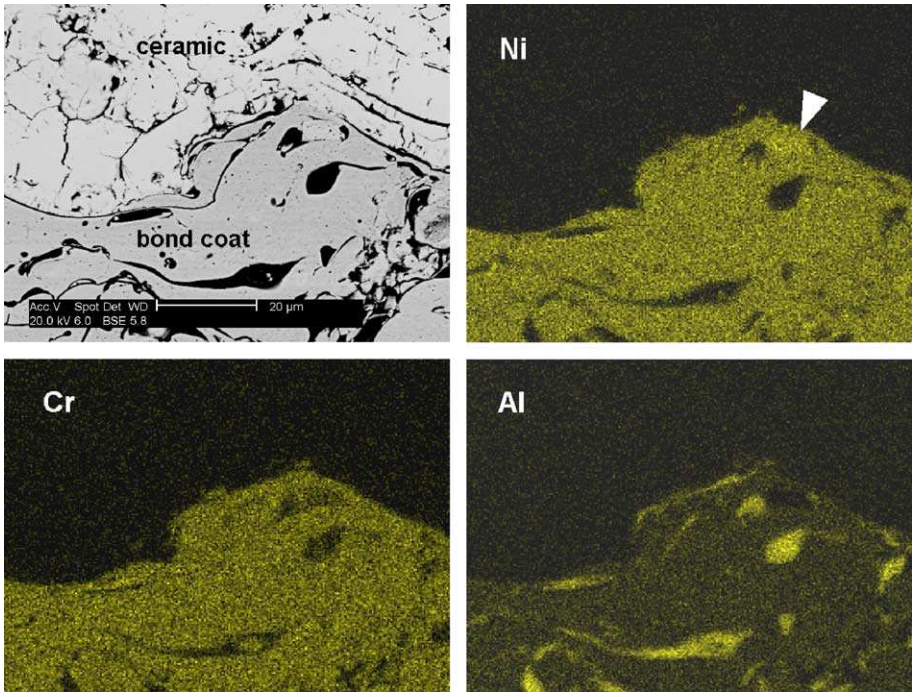

Fig. 1. Distribution of alloying elements in the NiCrAlY bond coat. The arrow indicates the segregation of nickel. SEM backscatter and digital X-ray images.

nucleation mechanism has not been clarified in relation to the formation of different components of the TGO. It has been reported that $Ni(Cr,Al)_2O_4$ (spinels) and NiO formed at above 1000 °C during the oxidation of thermal barrier coating systems [11,22–25]. It was suggested that these two oxides were detrimental to the durability of thermal barrier coating systems, because of the rapid local volume increase [24]. Hence, to gain a better understanding of the TBC failure mechanism, more attention needs to be paid to the detailed oxidation behaviors of the bond coat.

In the present study, for clarification of the role of certain oxides in causing crack nucleation and growth, TBC samples were tested in two different atmospheres: air and a low-pressure oxygen environment. By comparing the oxidation and crack formation behaviors of the TBC system in these two environments, the process of crack nucleation and propagation is further elucidated in relation to the formation of particular oxides in the bond coat of the TBC.

2. Experimental methods

The TBC samples were manufactured to consist of an yttria partially stabilized zirconia (ZrO_2–8%Y_2O_3) top coat and Ni–22Cr–10Al–1Y (wt.%) bond coat by plasma spraying in air onto 12.5-mm-diameter Inconel 625 substrate disks. The thickness of the ceramic coat is 250–310 μm, and that of the bond coat is 160–180 μm. Thermal exposure tests consisted of a 15-min ramp-up, 23-h isothermal soak at different temperatures from 930 to 1200 °C, and a 45-min cool-down to ambient temperature (25 °C). The low-pressure oxygen environment was prepared in quartz tubes, evacuated to a pressure of about 2×10^{-3} torr and backfilled with argon. The tested samples were examined using a Philips XL30S field emission gun scanning electron microscope (SEM) operating at an accelerating voltage between 5 and 20 kV.

3. Results

3.1. As-sprayed microstructure

The as-sprayed TBC was comprised of a ZrO_2–8%Y_2O_3 top coat and a Ni–22Cr–10Al–1Y (wt.%) bond coat. The

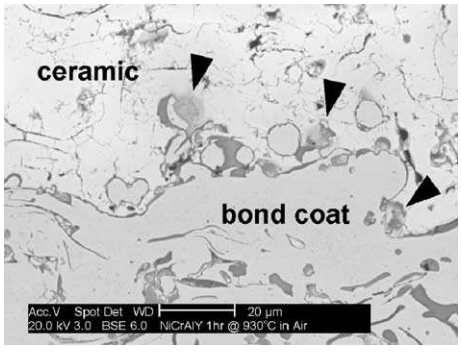

Fig. 2. Oxides formed in the original top coat/bond coat interface region after 1-h exposure at 930 °C in air. Arrows indicate mixed oxides of $(Cr,Al)_2O_3$, $Ni(Cr,Al)_2O_3$ and NiO. SEM backscatter image.

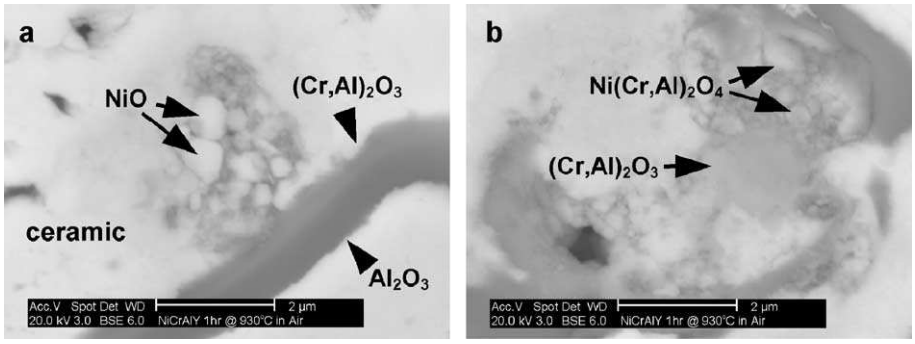

Fig. 3. Granular NiO and $Ni(Cr,Al)_2O_4$ particles between the ceramic and alumina layer after 1-h thermal exposure in air at 930 °C. SEM backscatter images.

ceramic coat contained porosity and some crack-like discontinuities, while the as-sprayed bond coat, although not fully dense, contained fewer such features. Aluminum was distributed nonuniformly in the bond coat (Fig. 1) because of pre-oxidation (formation of alumina) during the thermal spray processes. The aluminum concentration was found to be very low (<14 at.% or 7.5 wt.%) in some areas along the top coat/bond coat interface region. Nickel and chromium, on the other hand, were distributed rather uniformly in the bond coat. However, segregation of nickel still could be seen, as indicated by the arrow in Fig. 1.

3.2. Oxidation of NiCrAlY in air

Studies of the oxidation of the bond coat in air showed that after a 1-h exposure at a temperature of 930 °C, some relatively large oxide regions had formed, as indicated by the arrows in Fig. 2. The formation of a thin alumina (Al_2O_3) layer (~220 nm) between the ceramic top coat and the NiCrAlY bond coat could also be observed. Energy-dispersive spectrometer (EDS) analysis revealed that these massive oxides contained 15–45 at.% nickel, 8–24 at.% chromium and 2–30 at.% aluminum, while the Al_2O_3 layer contained >40 at.% Al, with <2 at.% Cr and <2 at.% Ni. The composition of the massive oxides was similar to that reported by other researchers [24,25]. These oxides appeared to be a mixture of chromia ($(Cr,Al)_2O_3$), spinels ($Ni(Cr,Al)_2O_4$) and nickel oxide (NiO) (Fig. 3). They formed in the Al_2O_3/ceramic top coat interface region. Moreover, a thin $(Cr,Al)_2O_3$ zone could also be observed between the Al_2O_3 layer and ceramic coat. For description purposes, these mixed oxides of chromia, spinel and nickel oxide are termed as $(Cr,Al)_2O_3 \cdot Ni(Cr,Al)_2O_4 \cdot NiO$, or abbreviated as CSN. As oxidation proceeded, the Al_2O_3 layer became thicker, which was ~1.1 μm after 100 h; however, the CSN region virtually did not grow as the exposure time increased (Fig. 4). The oxidation behavior of Ni–22Cr–10Al–1Y at 950 and 980 °C was practically the same as at 930 °C.

Upon thermal exposure in air at 1200 °C, the $(Cr,Al)_2O_3 \cdot Ni(Cr,Al)_2O_4 \cdot NiO$ grew more extensively in the TBC/bond coat interface region, as shown in Fig. 5, than at lower temperatures. The rapid growth of CSN caused crack nucleation in Figs. 5 and 6. Cracks usually nucleated within the $(Cr,Al)_2O_3 \cdot Ni(Cr,Al)_2O_4 \cdot NiO$ (Figs. 5a and 6a) and grew into the ceramic top coat. Sometimes, they also formed at the interface between the ceramic top coat and Al_2O_3 layer where a layer of $(Cr,Al)_2O_3$ was present (Fig. 5b). At a later stage, these interfacial cracks coalesced to form a long dominant crack in the ceramic top coat near the interface (Fig. 6b) in a cleavage mode, leading to TBC separation from the bond coat after 161 h (Fig. 7). The feature of this later stage of crack propagation has been widely observed [9–12]. On the other hand, crack

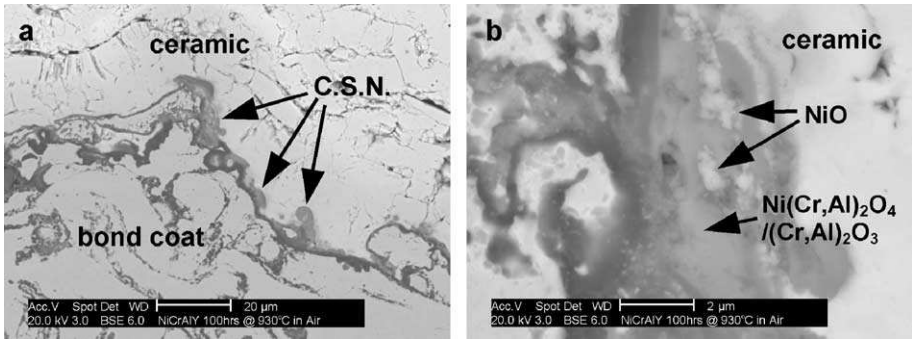

Fig. 4. Heterogeneously distributed $(Cr,Al)_2O_3 \cdot Ni(Cr,Al)_2O_4 \cdot NiO$ between the Al_2O_3 layer and ceramic top coat (a) after 100 h at 930 °C. The figure in (b) is a close-up look of CSN in (a). SEM backscatter images.

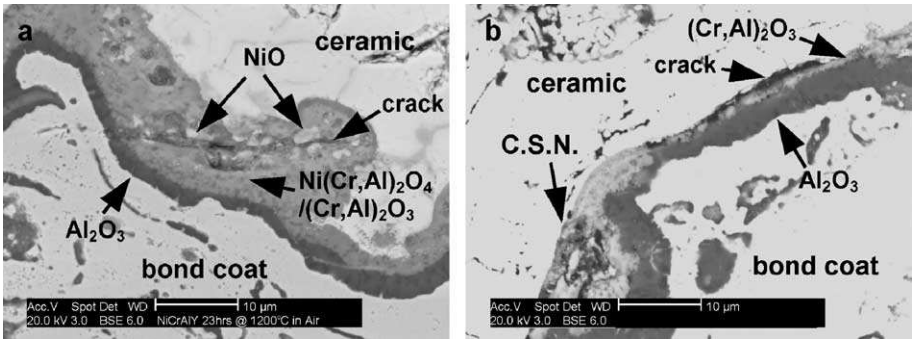

Fig. 5. Crack nucleation via void formation in $(Cr,Al)_2O_3 \cdot Ni(Cr,Al)_2O_4 \cdot NiO$ (a) and at the interface between ceramic top coat and $(Cr,Al)_2O_3$ (b) after 23 h in air at 1200 °C. SEM backscatter images.

propagation related to the formation of an Al_2O_3 layer was rather limited.

The formation of $(Cr,Al)_2O_3 \cdot Ni(Cr,Al)_2O_4 \cdot NiO$-mixed oxides was quite heterogeneous, as shown in the micrographs of Figs. 5–7. Therefore, their growth kinetics were difficult to quantify. Generally speaking, the higher the temperature, the greater the volume of $(Cr,Al)_2O_3 \cdot Ni(Cr,Al)_2O_4 \cdot NiO$ formed, but once formed at a particular temperature (at least above 930 °C), the CSN volume fraction did not seem to change with exposure time. On the other hand, the Al_2O_3 layer formed rather uniformly along the original interface between the ceramic and the bond coat, and its thickness increased monotonically with exposure time, as shown in Fig. 8a. The behavior of Al_2O_3 thickening roughly followed a parabolic function of time, as further demonstrated in Fig. 8b. This is consistent with a diffusion-controlled thickening process, where the relationship between the thickness (δ) and exposure time (t) is expected to be $\delta^2 \propto t$. Thus, thickening of Al_2O_3 layer can be described as

$$d\delta^2_{Al_2O_3}/dt = 2k_0 e^{-Q/RT}$$

where k_0 is a constant, Q is the activation energy for the Al_2O_3 layer growth, R is the universal gas constant and T is the bond coat temperature, since oxidation is a thermally activated process. The Arrhenius plot of Al_2O_3 layer thickening (Fig. 9) gives an activation energy of $Q \approx 188$ kJ/mol for the present NiCrAlY bond coat. Meier and co-workers [13] obtained an activation energy of about 231 kJ/mol for the thickening of oxide layer in their study.

3.3. Oxidation of NiCrAlY in the low-pressure oxygen condition

When exposed for 161 h at 1200 °C in a low-pressure condition (~2×10^{-3} torr), a thin Al_2O_3 layer of about 3–5 μm thick formed at the interface between the ceramic top coat and metallic bond coat, with limited formation of $Ni(Cr,Al)_2O_4$ and NiO. The number of cracks formed in association with the growth of the alumina layer in the interfacial region was very limited, although a few could be identified at the interface between the Al_2O_3 layer and bond coat as indicated by arrows (Fig. 10). Crack propagation did occur in the ceramic top coat (some might have penetrated the Al_2O_3 layer), primarily via the coalescence of pre-existing flaws; nevertheless, the mode did not appear to be the cleavage type, as in air. However, after 299 h in the low-pressure oxygen environment, some sintering of the ceramic top coat had taken place, and separation of the TBC occurred within the degraded bond coat near the bond coat/substrate interface (Fig. 11a). At this time, it was observed

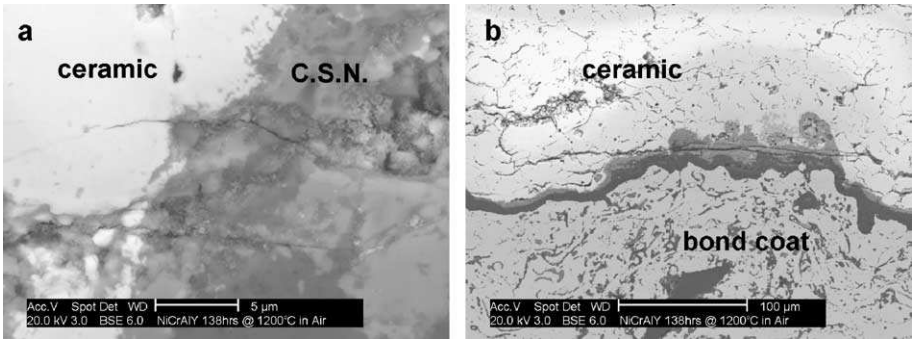

Fig. 6. Crack nucleated in $(Cr,Al)_2O_3 \cdot Ni(Cr,Al)_2O_4 \cdot NiO$ grows into ceramic (a) and crack propagation in the interface region (b). After 138 h in air at 1200 °C. SEM backscatter images.

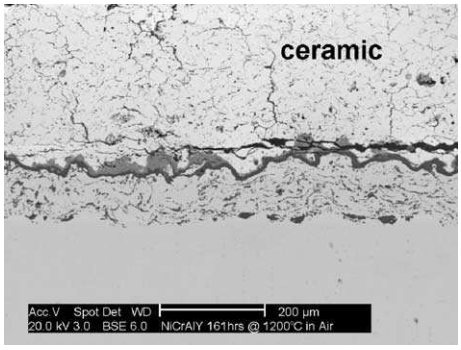

Fig. 7. TBC separation after 161 h as a result of coalescence of the interfacial cracks and preexisting flaws and cleavage crack growth in the ceramic. SEM backscatter image.

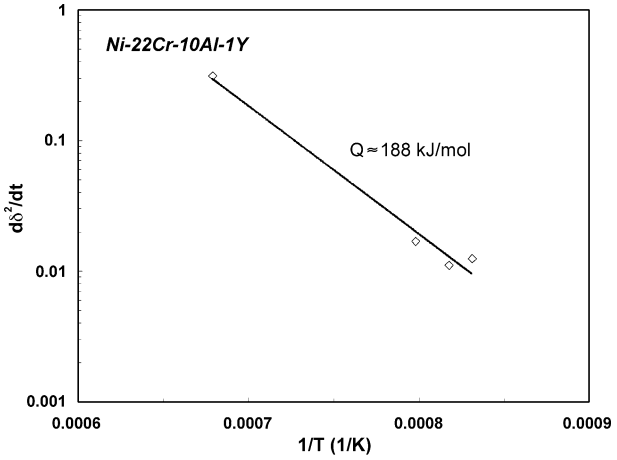

Fig. 9. Arrhenius plot for Al_2O_3 layer growth between 930 and 1200 °C.

that the Al_2O_3 layer dissolved, and the bond coat was further oxidized, via the formation of finer $Ni(Cr,Al)_2O_4$ (Fig. 11b), an observation similar to that made by Shillington and Clarke [23].

4. Discussion

The formation of spinel ($Ni(Cr,Al)_2O_4$) and NiO at the interface between the ceramic coat and Al_2O_3 layer has been reported by many researchers [11,22–25]. It has been suggested that below 1000 °C, one of the possible causes of spinel formation between the ceramic coat and the Al_2O_3 layer in an EB-PVD-produced TBC system is transportation of nickel through the Al_2O_3 layer [3], since thermodynamic considerations indicate that Al_2O_3 would tend to form first in NiCrAlY bond coats [3,26]. In the present study, $(Cr,Al)_2O_3 \cdot Ni(Cr,Al)_2O_4 \cdot NiO$ oxides were observed even after only a 1-h thermal exposure in air at 930 °C (Fig. 3b). It was noted, as well, that these oxides did not grow during later extended thermal exposure (Fig. 4). It is thus postulated that these $(Cr,Al)_2O_3 \cdot Ni(Cr,Al)_2O_4 \cdot NiO$ oxides formed in the very beginning of the oxidation process. This occurred at sites where the aluminum concentration was low and nickel had segregated as a result of compositional inhomogeneity in the air-plasma-sprayed (APS) TBC system. These zones were situated along the original ceramic/bond coat interface region (Fig. 1), and it is believed that the mixed oxides were produced because locally, there was insufficient aluminum reacting to form an initial alumina layer to serve as an effective diffusion barrier to nickel.

In the low-pressure oxygen environment, however, formation of $(Cr,Al)_2O_3 \cdot Ni(Cr,Al)_2O_4 \cdot NiO$-mixed oxides was very limited, even though the longer life of the TBC under this condition resulted in an increase in the exposure time at high temperature and, hence, the time available for nickel transportation to occur. Comparing the $(Cr,Al)_2O_3 \cdot Ni(Cr,Al)_2O_4 \cdot NiO$ formation in the two environments, it can be concluded that compositional inhomogeneity and oxygen pressure may play a more important role in the $(Cr,Al)_2O_3 \cdot Ni(Cr,Al)_2O_4 \cdot NiO$ for-

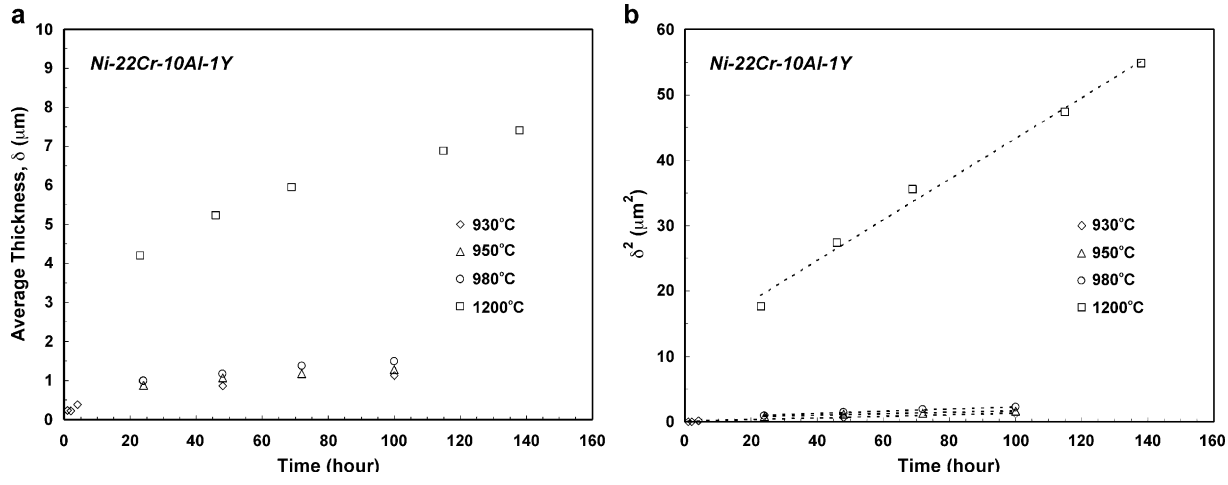

Fig. 8. Average thickness of Al_2O_3 layer, δ, as a function of exposure time at various temperatures (a) and relationship between δ^2 and time (b).

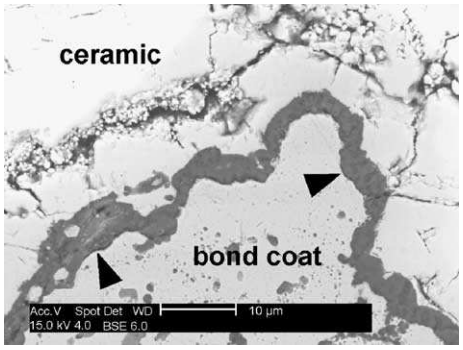

Fig. 10. Limited amount of cracks can be observed at the interface between Al_2O_3 layer and bond coat after 161 h in low-pressure oxygen condition. SEM backscatter image.

mation than nickel transportation via diffusion in air-plasma-sprayed TBC systems.

The formation of $(Cr,Al)_2O_3 \cdot Ni(Cr,Al)_2O_4 \cdot NiO$ in air usually proceeded via the development of $(Cr,Al)_2O_3$ containing embedded $Ni(Cr,Al)_2O_4$ and NiO particles (Figs. 3 and 4) and cracks nucleated within the $(Cr,Al)_2O_3 \cdot Ni(Cr,Al)_2O_4 \cdot NiO$ or at the interface between the ceramic and $(Cr,Al)_2O_3$ (Fig. 5). It is likely that the fast growth of $Ni(Cr,Al)_2O_4$ and NiO [24] resulted in a stress buildup at the $Ni(Cr,Al)_2O_4/(Cr,Al)_2O_3$ and $NiO/(Cr,Al)_2O_3$ interfaces, leading to crack nucleation within the $(Cr,Al)_2O_3 \cdot Ni(Cr,Al)_2O_4 \cdot NiO$ (Fig. 5) and growth into the ceramic coat in a cleavage mode (Fig. 6a). In contrast, $(Cr,Al)_2O_3 \cdot Ni(Cr,Al)_2O_4 \cdot NiO$ oxides were practically absent in the low-pressure oxygen-exposed TBC and crack formation was very limited, albeit a layer of Al_2O_3 still formed along the ceramic/bond coat interface. Here, it should also be mentioned that the thermal mismatch strains between the ceramic and bond coat would still exist and be identical in the TBC coupons subjected to the same thermal cycle but in different environments. Therefore, it may be postulated that bond coat oxidation plays a critical role in causing crack nucleation and subsequent growth. Thus, depending on the type and amount of oxides formed in a bond coat, the TBC spallation behavior can be quite different. As such, it can be anticipated that, upon thermal exposure in air, the $(Cr,Al)_2O_3 \cdot Ni(Cr,Al)_2O_4 \cdot NiO$ forms rapidly in areas with low aluminum concentration, along the original ceramic/bond coat interface, while the Al_2O_3 layer starts to form. Cracks most likely initiate within the $(Cr,Al)_2O_3 \cdot Ni(Cr,Al)_2O_4 \cdot NiO$ or at the interface between the ceramic and $(Cr,Al)_2O_3$ and grow into the ceramic top coat in a cleavage mode. The coalescence of these cracks, as well as the pre-existing flaws within the ceramic coat, would take place at a later stage, resulting in long cracks, which might become the dominant ones causing spallation of TBC from the bond coat. Whereas some other studies attributed the root cause of failure to the TGO as a whole [9–12], the present study provides a detailed description of the crack nucleation mechanisms, via the formation of $(Cr,Al)_2O_3 \cdot Ni(Cr,Al)_2O_4 \cdot NiO$. The actual crack sizes have been found to follow log-normal distributions, as reported elsewhere [27]. By comparing the TBC cracking behavior in air with that in an inert environment, where the TBC life is almost double that in air, it is shown that the Al_2O_3 is not as detrimental to TBC life as $(Cr,Al)_2O_3 \cdot Ni(Cr,Al)_2O_4 \cdot NiO$. Therefore, it can be expected that reducing the amount of $(Cr,Al)_2O_3 \cdot Ni(Cr,Al)_2O_4 \cdot NiO$ at the interface between the ceramic and Al_2O_3 layer may lead to an extended TBC life.

5. Conclusions

Oxidation behaviour of a Ni–22Cr–10Al–1Y bond coat at temperatures between 930 and 1200 °C and in two environments, air and a low-pressure oxygen condition, was investigated. The major findings on the oxidation behavior in relation to crack nucleation and growth can be summarized as follows:

Mixed oxides, $(Cr,Al)_2O_3 \cdot Ni(Cr,Al)_2O_4 \cdot NiO$, formed in the very beginning of the thermal exposure in air, along with the formation of the Al_2O_3 layer. This is considered to result from the segregation of Ni in the interfacial region between the ceramic coat and NiCrAlY bond coat.

Cracks initiated mostly in association with the formation of $(Cr,Al)_2O_3 \cdot Ni(Cr,Al)_2O_4 \cdot NiO$. In particular, Ni $(Cr,Al)_2O_4$ and NiO particles embedded in chromia could act as crack nuclei. Upon the volumetric change induced by

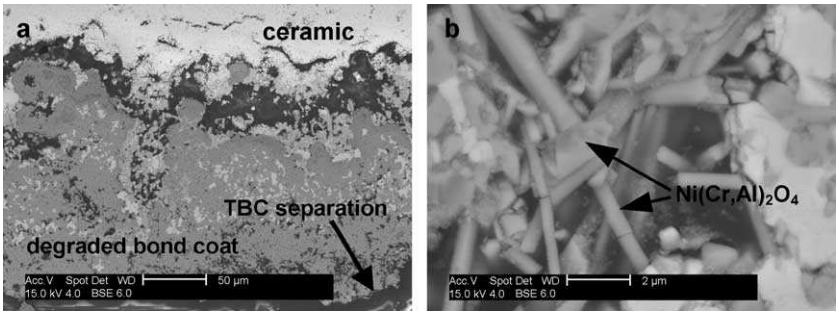

Fig. 11. TBC failed after 299 h in low-pressure condition, after sintering of ceramic coat (a) and degradation of bond coat (b) occurred. SEM backscatter images.

the oxidation, cracks thus formed were driven into the ceramic coat and grew in a cleavage mode, leading to the separation of the TBC. Whereas in the low-pressure oxygen-exposed TBC, where the mixed oxides were practically absent, crack formation was very limited, and the TBC failed by total degradation of the bond coat.

Acknowledgements

The authors are grateful to the Department of National Defence Canada and the SURFTEC consortium for their partial support.

References

[1] G.W. Goward, Surface and Coatings Technology 108–109 (1998) 73.
[2] A. Bennett, Materials Science and Technology 2 (1986) 257.
[3] M.J. Stiger, N.M. Yanar, M.G. Topping, F.S. Pettit, G.H. Meier, Zeitschrift fur Metallkund 90 (1999) 1069.
[4] Z.A. Chaudhury, G.M. Newaz, S.Q. Nusier, T. Ahmed, Materials Science and Engineering A231 (1997) 34.
[5] M. Tamura, M. Takhashi, J. Ishii, K. Suzuki, M. Sato, K. Shimomura, Journal of Thermal Spray Technology 8 (1) (1999) 68.
[6] N. Czech, H. Fietzek, M. Juez-Lorenzo, V. Kolarik, W. Stamm, Surface and Coatings Technology 113 (1999) 157.
[7] P.K. Wright, A.G. Evans, Current Opinion in Solid State and Materials Science 4 (1999) 255.
[8] H.E. Evans, M.P. Taylor, Oxidation of Metals 55 (1–2) (2001) 17.
[9] R.A. Miller, C.E. Lowell, Thin Solid Films 95 (1982) 265.
[10] J.T. DeMasi-Marcin, K.D. Sheffler, S. Bose, ASME Paper 89-GT-132 (1989).
[11] A. Rabiei, A.G. Evans, Acta Materialia 48 (2000) 3963.
[12] E.P. Busso, J. Lin, S. Sakurai, Acta Materialia 49 (2001) 1529.
[13] S.M. Meier, D.M. Nissley, K.D. Sheffler, T.A. Cruse, Transactions of the ASME 114 (1992) 258.
[14] M. Gell, E. Jordan, K. Vaidyanathan, K. McCarron, B. Barber, Y-H. Sohn, V.K. Tolpygo, Surface and Coatings Technology 120–121 (1999) 53.
[15] C. Funke, J.C. Mailand, B. Siebert, R. Vaβen, D. Stöver, Surface and Coatings Technology 94–95 (1997) 106.
[16] G.M. Newaz, Damage Accumulation Mechanisms in Thermal Barrier Coatings, Wayne State University Technical Report, AFRL-SR-BL-TR-98-0592.
[17] S. Nusier, G. Newaz, Engineering Fracture Mechanics 60 (1998) 577.
[18] A.G. Evans, J.W. Hutchinson, Y. Wei, Acta Materialia 47 (1999) 4093.
[19] M. Pindera, J. Aboudi, S.M. Arnold, Materials Science and Engineering A284 (2000) 158.
[20] E.P. Busso, J. Lin, S. Sakurai, M. Nakayama, Acta Materialia 49 (2001) 1515.
[21] A.M. Limarga, S. Widjaja, T.H. Yip, L.K. Teh, Surface and Coatings Technology 153 (2002) 16.
[22] J.A. Haynes, E.D. Rigney, M.K. Ferber, W.D. Porter, Surface and Coatings Technology 86–87 (1996) 102.
[23] E.A.G. Shillington, D.R. Clarke, Acta Materialia 47 (1999) 1297.
[24] C.H. Lee, H.K. Kim, H.S. Choi, H.S. Ahn, Surface and Coatings Technology 124 (2000) 1.
[25] L. Ajdelsztajn, J.A. Picas, G.E. Kim, F.L. Bastian, J. Schoenung, V. Provenzano, Materials Science and Engineering A338 (2002) 33.
[26] F.S. Pettit, G.H. Meier, Superalloys (1984) 651.
[27] X.J. Wu, P.C. Patnaik, M. Liao, and W.R. Chen, A Statistical Assessment of the Damage State in Plasma-Sprayed Thermal Barrier Coating, Technical Conference of ASME TURBO EXPO 2003, Atlanta, Georgia, June 16–19, 2003.